

# Supporting Information

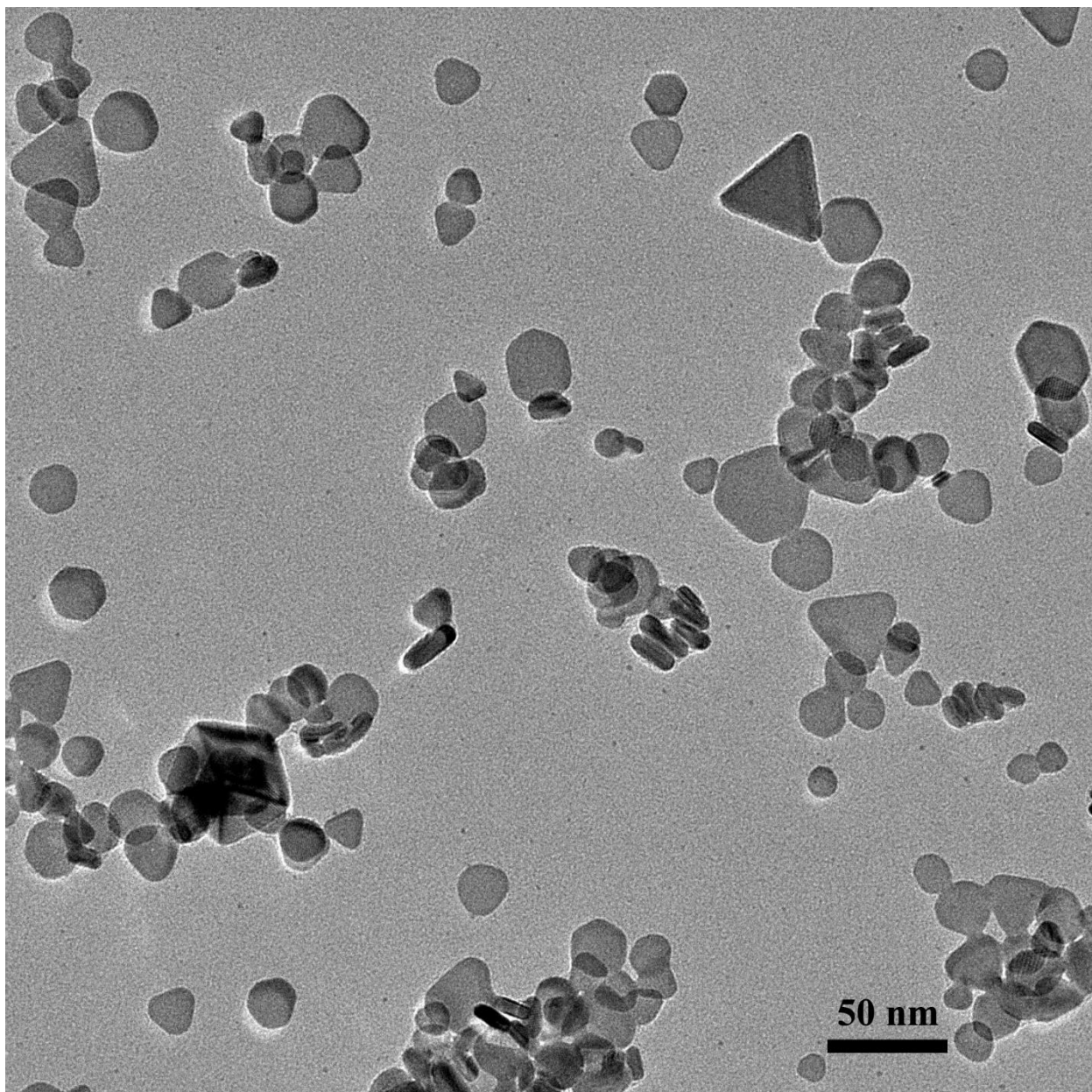


Figure S1. TEM images of Ag nanoplate seeds with rounded triangular shape. The average diameter along the lateral direction is about 25nm. The thickness is near 7nm.



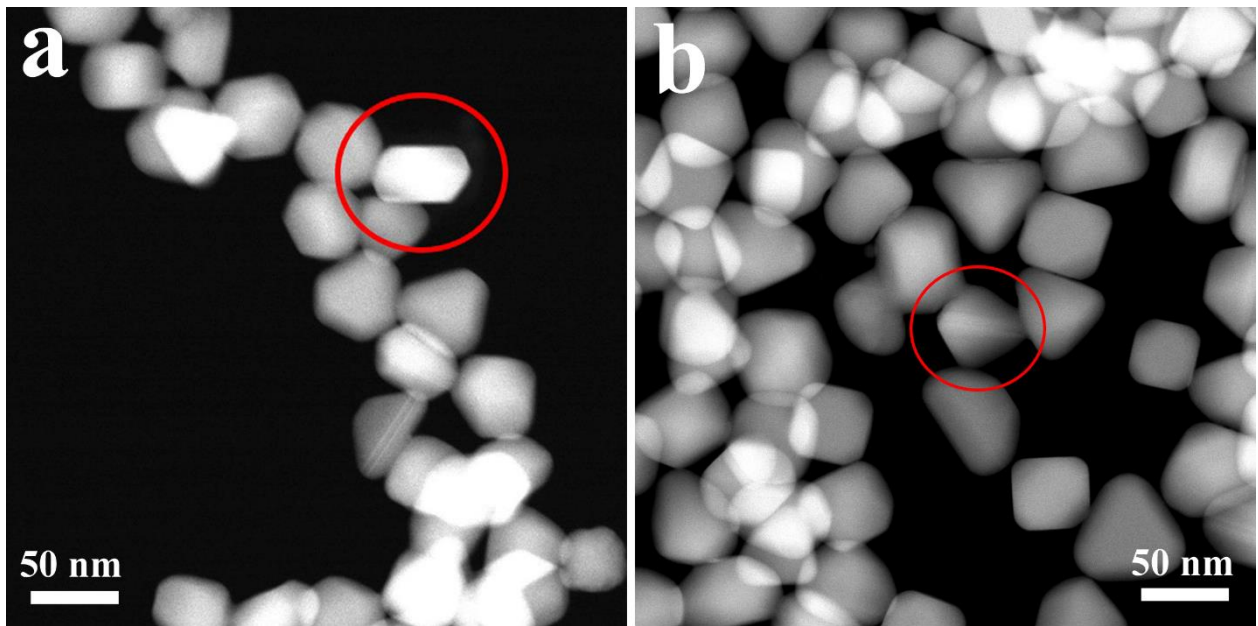


Figure S4. HAADF image of hexagonal nanoplates (truncated cube) and truncated bipyramid obtained from vertical growth of round nanoplates seeds with 2mL  $\text{AgNO}_3$ . The particles tabbed by cycle are standing on the carbon film oriented at  $\langle 10\bar{1} \rangle$  direction, which are favorable to detect the defect structure directly.

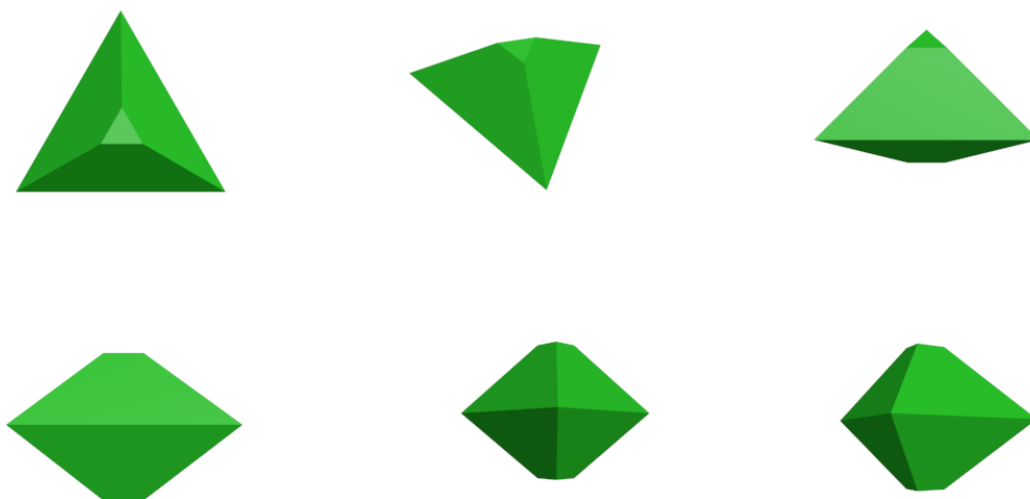


Figure S5. Simulations of truncated bipyramid viewed from different directions.

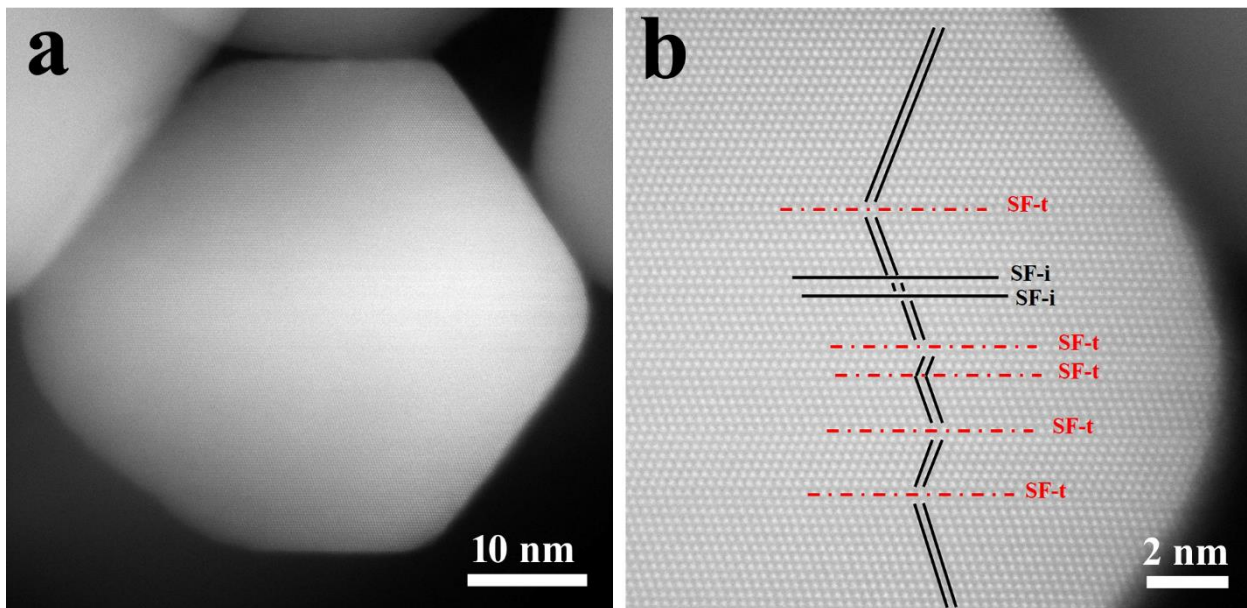


Figure S6. HAADF image of a truncated bipyramid with 5 SF-t and 2 SF-i.

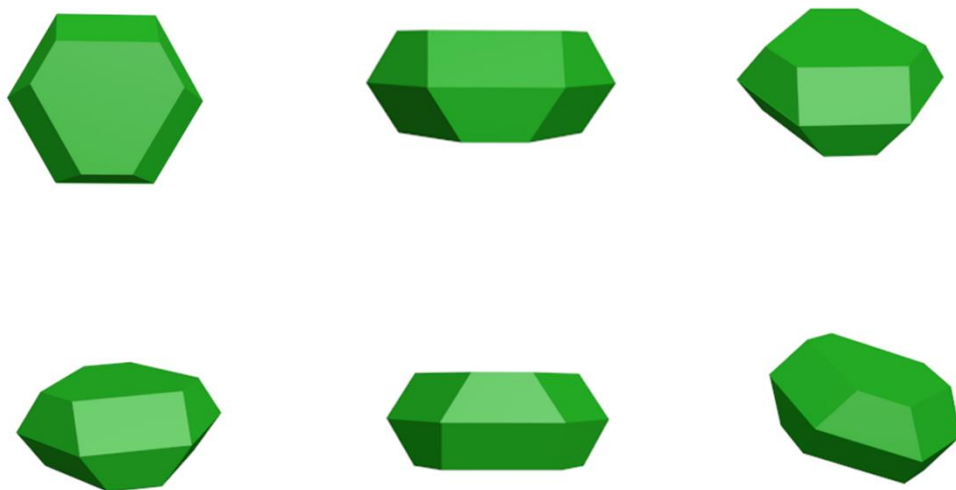


Figure S7. Simulations of thick hexagonal nanoplate viewed from different directions.



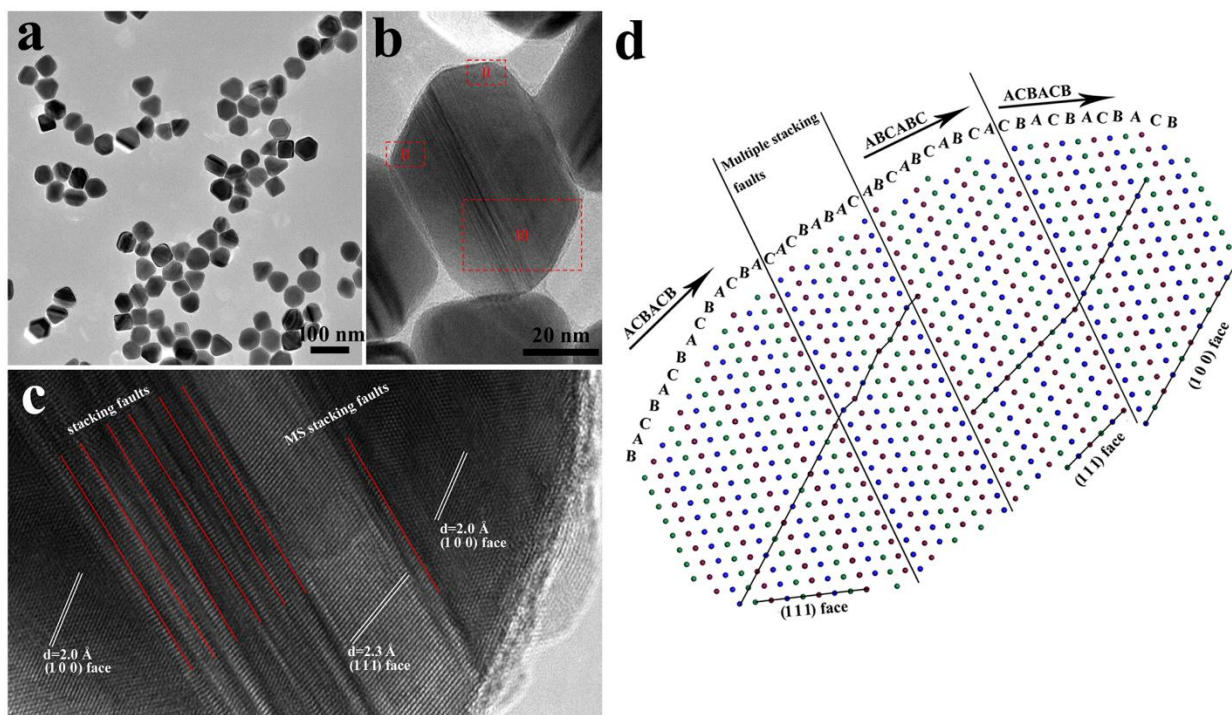


Figure S8. TEM image of hexagonal nanoplates (truncated cube) and truncated bipyramid obtained from vertical growth of round nanoplates seeds with 2mL  $\text{AgNO}_3$ . (a) (b) TEM image, (c) High resolution TEM image, (d) lattice simulation.

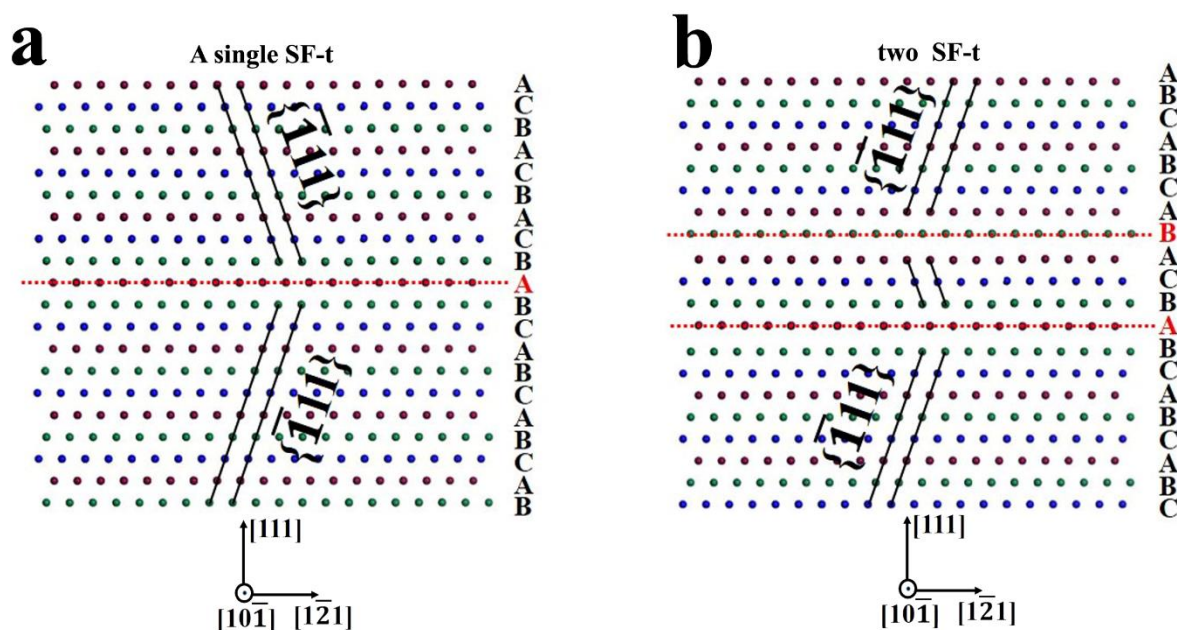


Figure S9. Simulation of the lattice arrangements with (a) a single SF-t and (b) two SF-t. A single twinned stacking faults makes the  $\{111\}$  facets change their extending directions. (a) The orientations of  $\langle 111 \rangle$  faces above and below the SF-t are mirrored by the planar defective layer, indicating mirror symmetry. (b) The orientations of  $\langle 111 \rangle$  faces above and below the layer of two SF-t extend to the same direction, suggesting center symmetry.

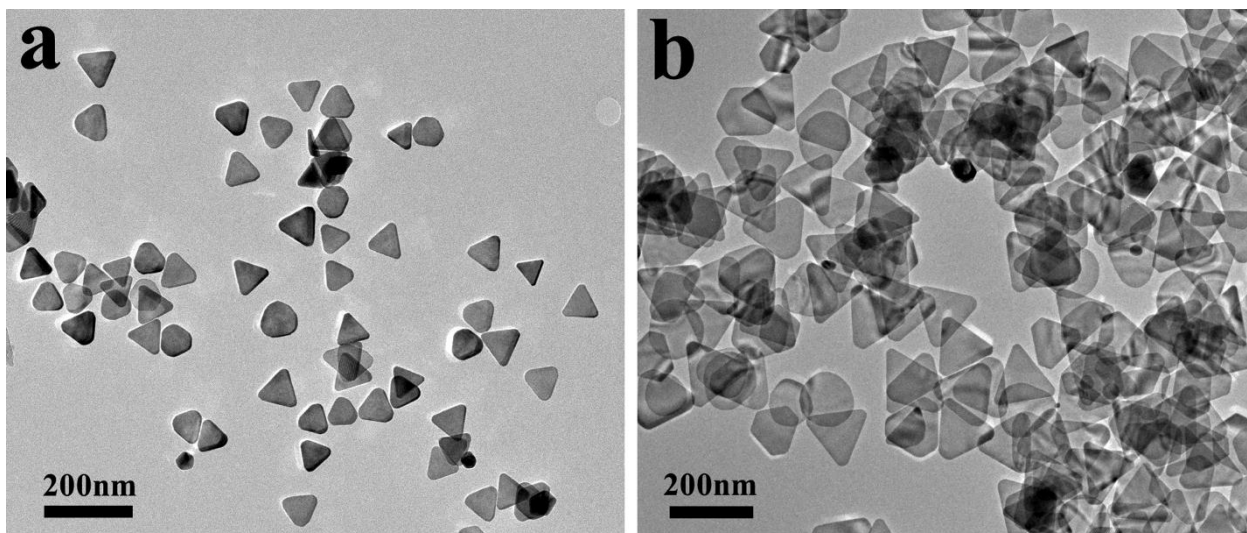


Figure S10. Triangular nanoplates obtained from lateral growth. (a) Growth with adding 1 mL and (b) 2 mL  $\text{AgNO}_3$  in the presence of  $\text{CuSO}_4$ . The average diameters in (a) and (b) are 78 nm and 130 nm, respectively.

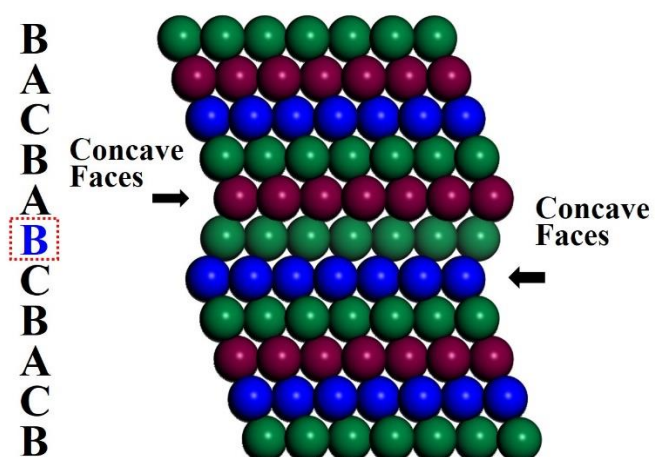


Figure S11. Simulations of concave faces formed in SF-i. The concave faces are (111) face.

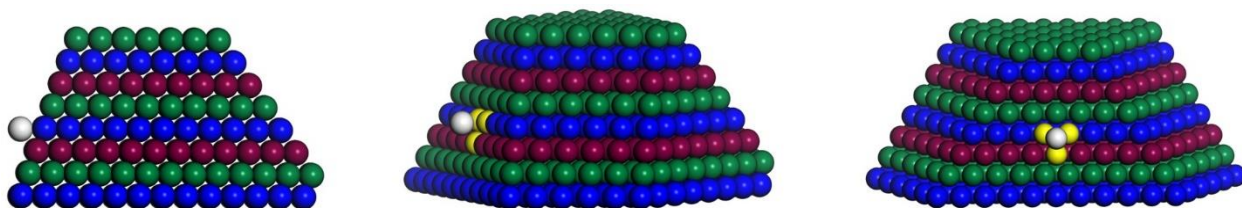


Figure S12. Simulations of adding atom on the (111) face with a coordination number of 3.



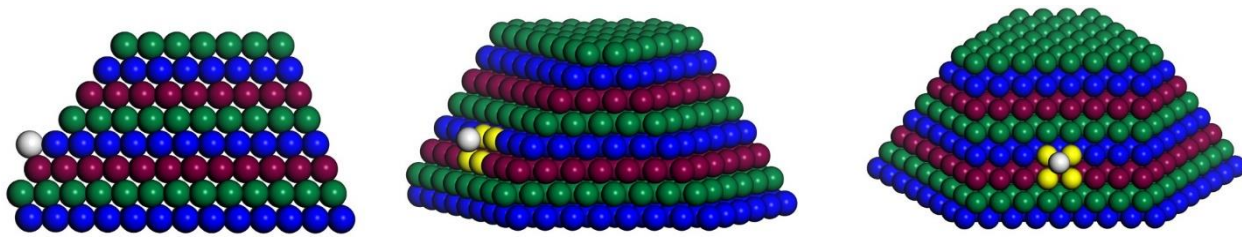
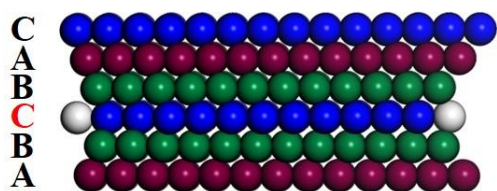
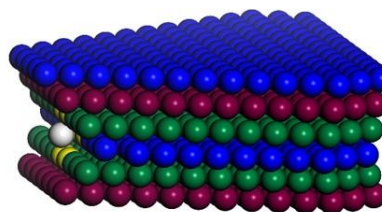


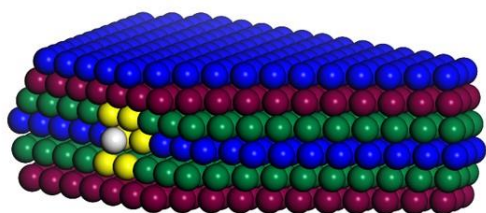
Figure S13. Simulations of adding atom on the (100) face with a coordination number of 4.



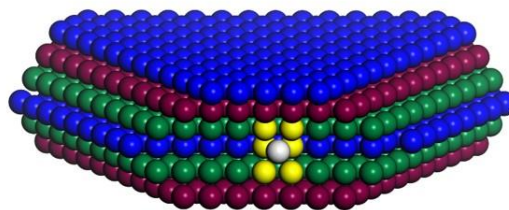
**Side direction**



**Side direction**



**Side direction**



**Front direction**

Figure S14. Simulations of adding atom on the surface of SF-t. The coordination number of the adding atom is 6 at the defect site.



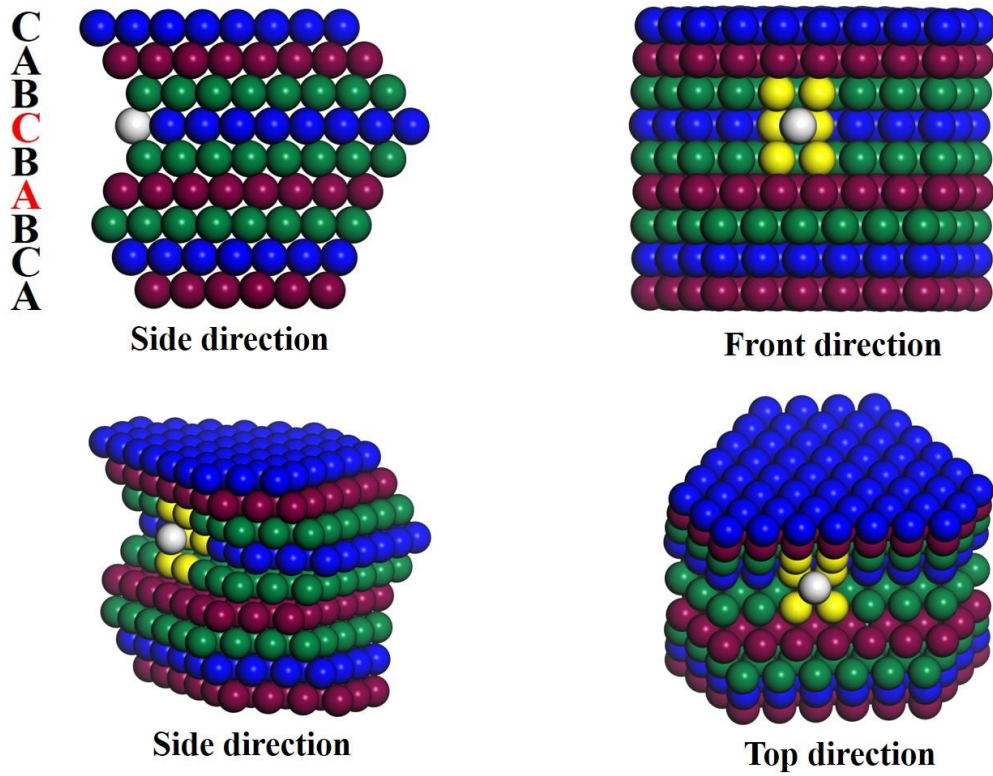


Figure S15. Simulations of adding atom on the surface of SF-i. The coordination number of the adding atom is 6 at the defect site.

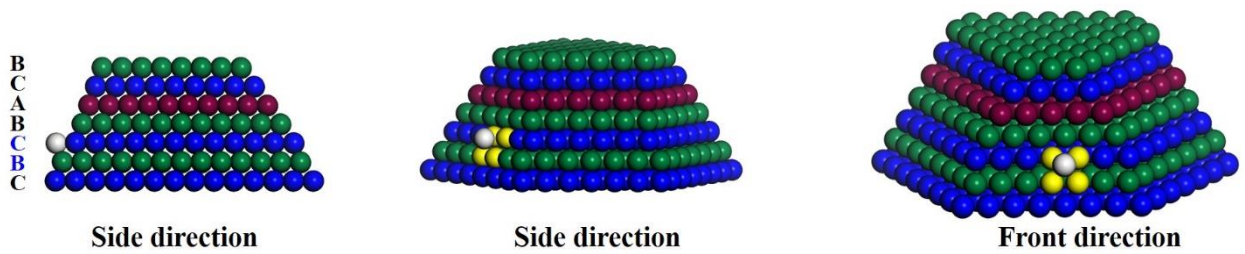


Figure S16. Simulations of adding atom on the surface of SF-m. The coordination number of the adding atom is 4 at the defect site.

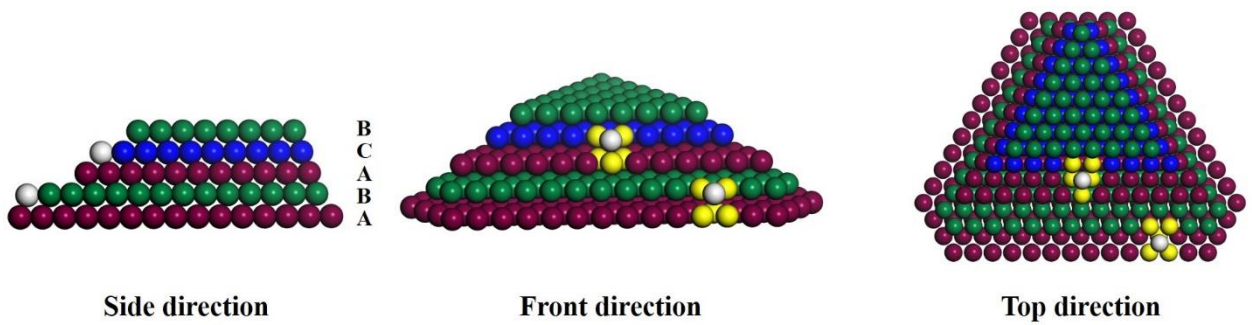


Figure S17. Simulations of adding atom on the step faces. The coordination number of the adding atom is 5 at the step sites.

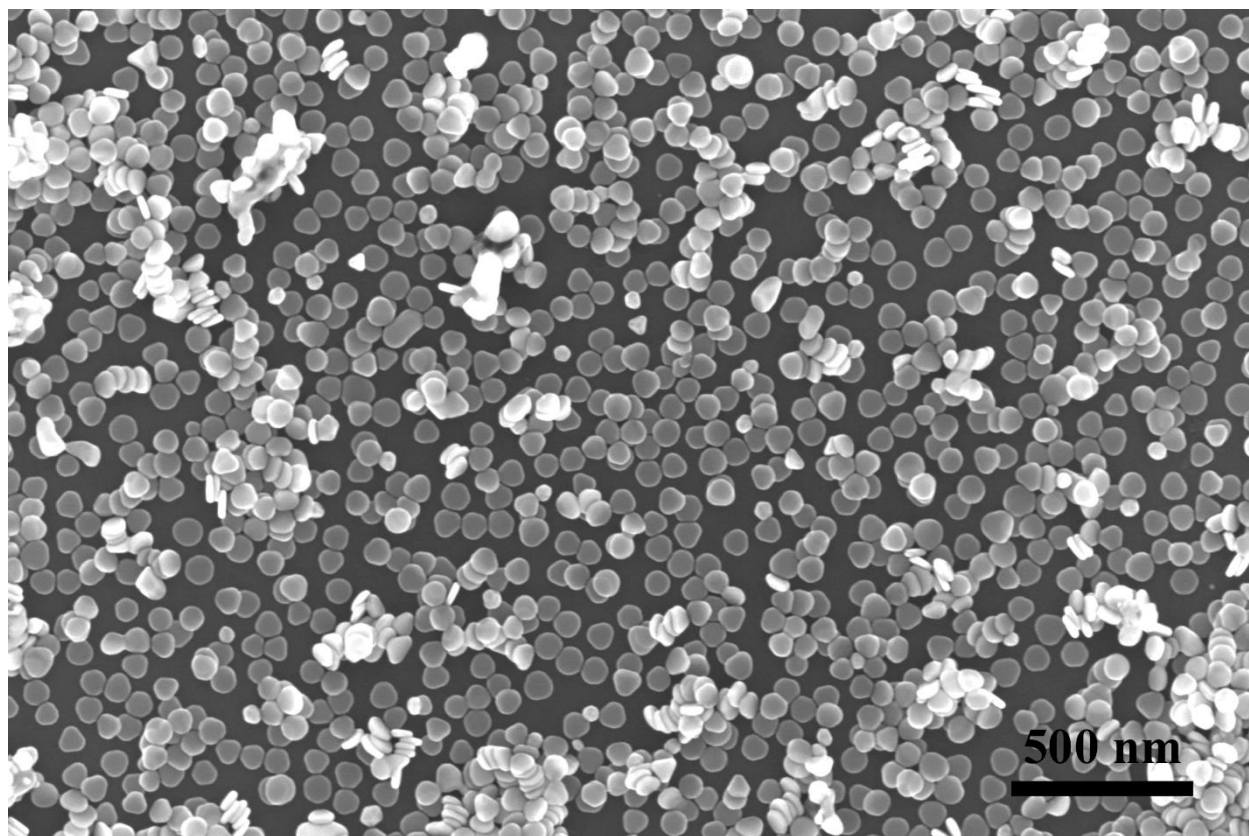


Figure S18. SEM image of silver nanoplates after vertical growth of 0.25mL  $\text{AgNO}_3$  by using triangular silver nanoplate (78nm in length) as seeds. The average length and thickness of the nanoplates were 68 and 19nm, respectively.

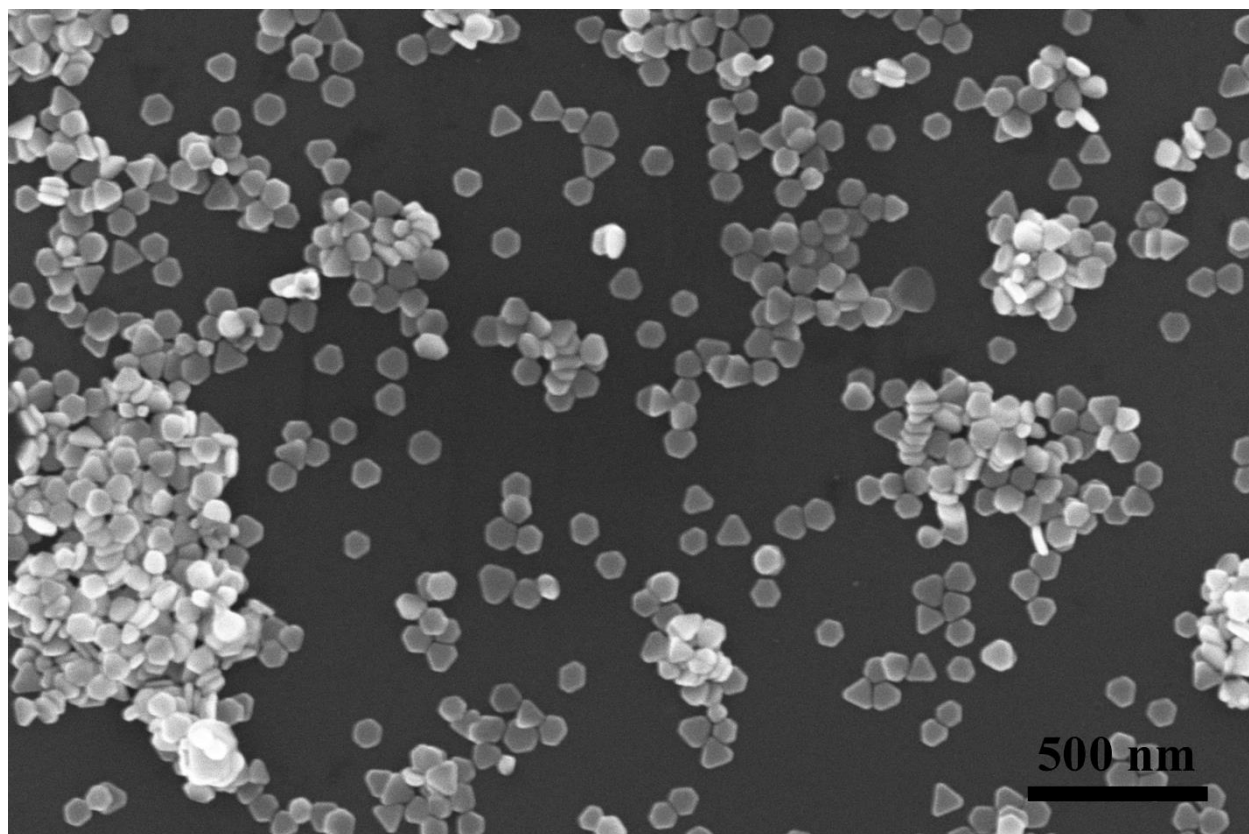


Figure S19. SEM image of silver nanoplates after vertical growth of 0.50 mL  $\text{AgNO}_3$  by using triangular silver nanoplate (78nm in length) as seeds. The average length and thickness of the nanoplates were 77nm and 26nm, respectively.



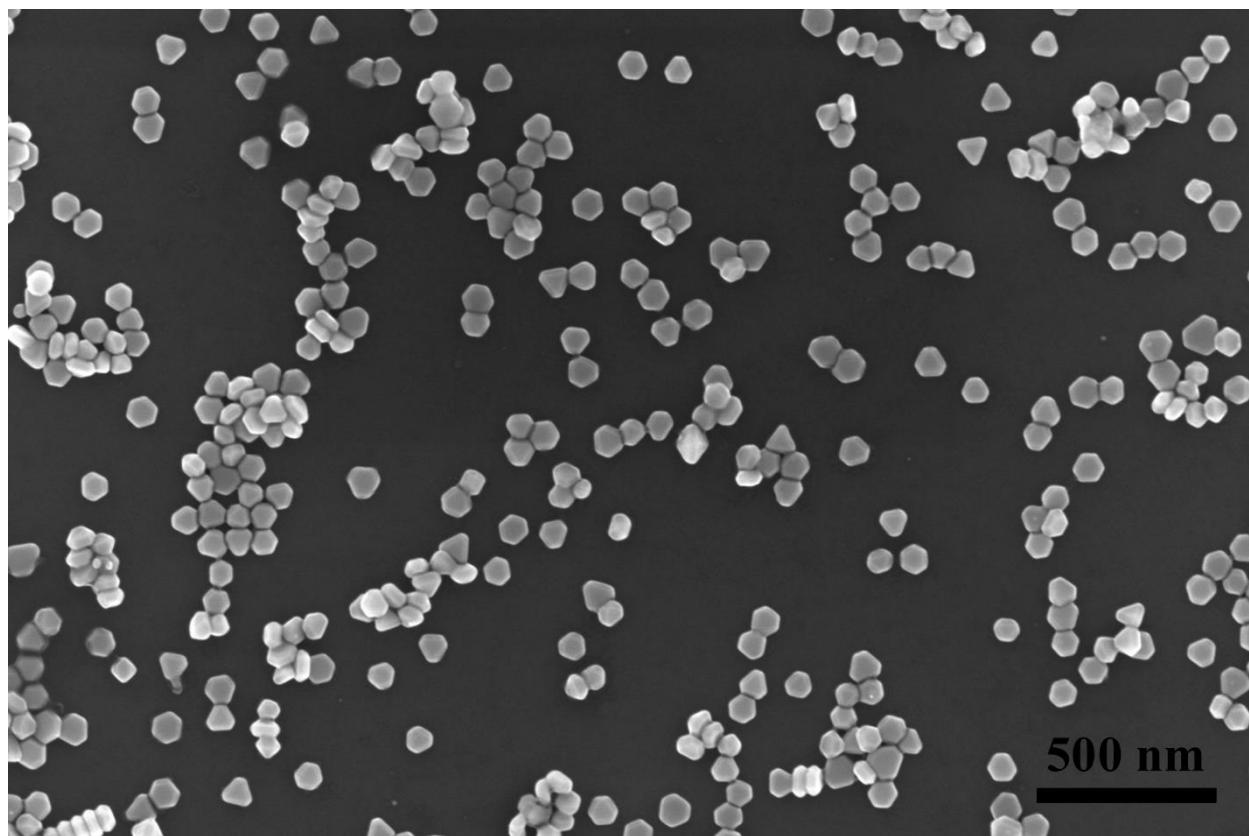


Figure S20. SEM image of silver nanoplates after vertical growth of 1.0 mL  $\text{AgNO}_3$  by using triangular silver nanoplate (78nm in length) as seeds. The average length and thickness of the nanoplates were 77nm and 41nm, respectively.

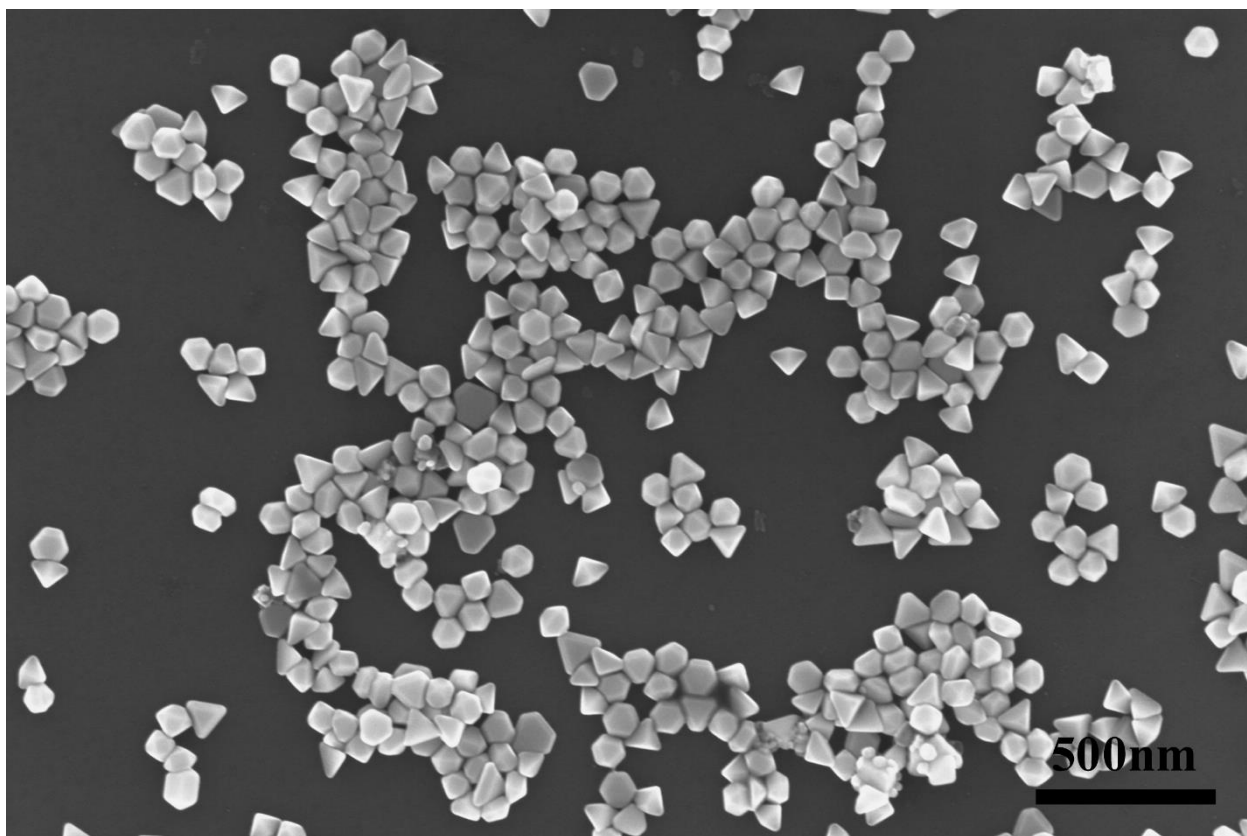


Figure S21. SEM image of silver nanoplates after vertical growth of 2.0 mL  $\text{AgNO}_3$  by using triangular silver nanoplate (78nm in length) as seeds. The average length and thickness of the nanoplates were 90nm and 70nm, respectively.

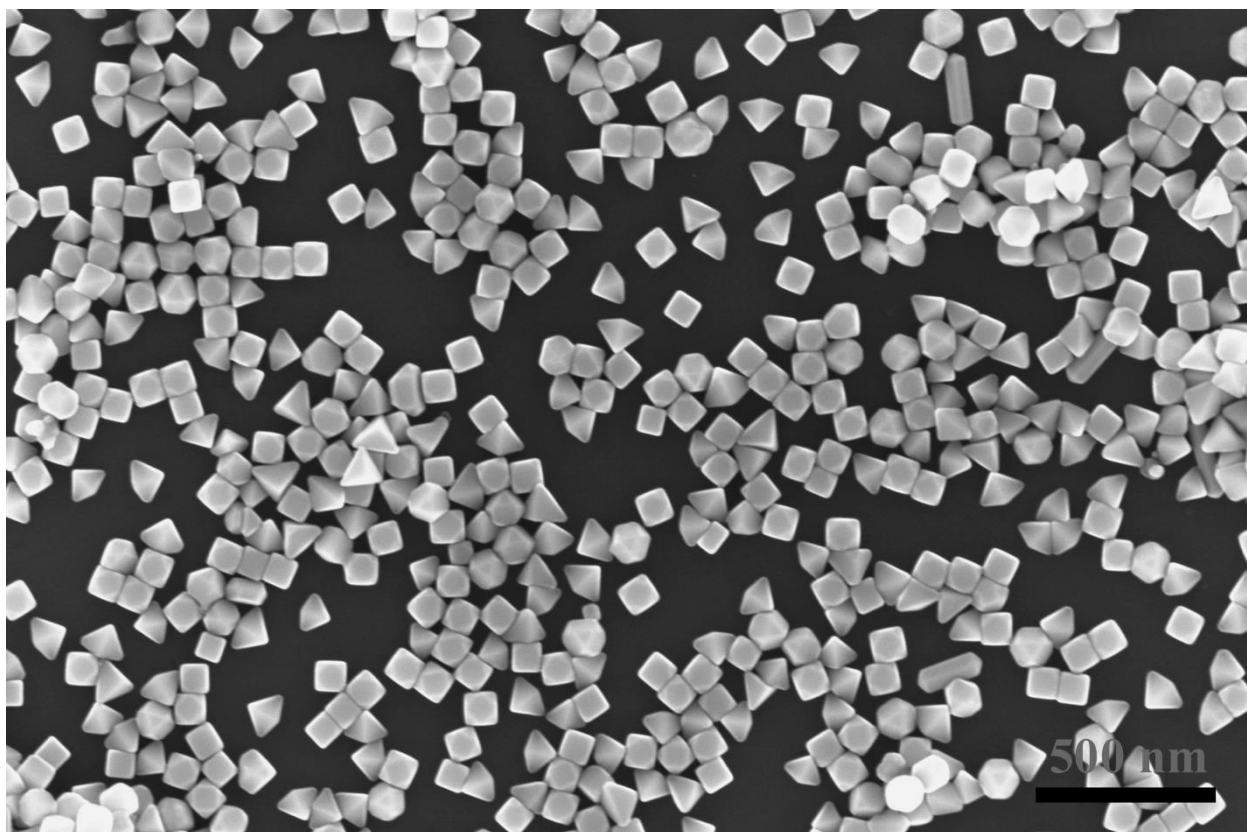


Figure S22. SEM image of silver nanoplates after vertical growth of 4.0 mL  $\text{AgNO}_3$  by using triangular silver nanoplate (78nm in length) as seeds. The average length and thickness of the nanoplates were 110nm and 100nm, respectively.



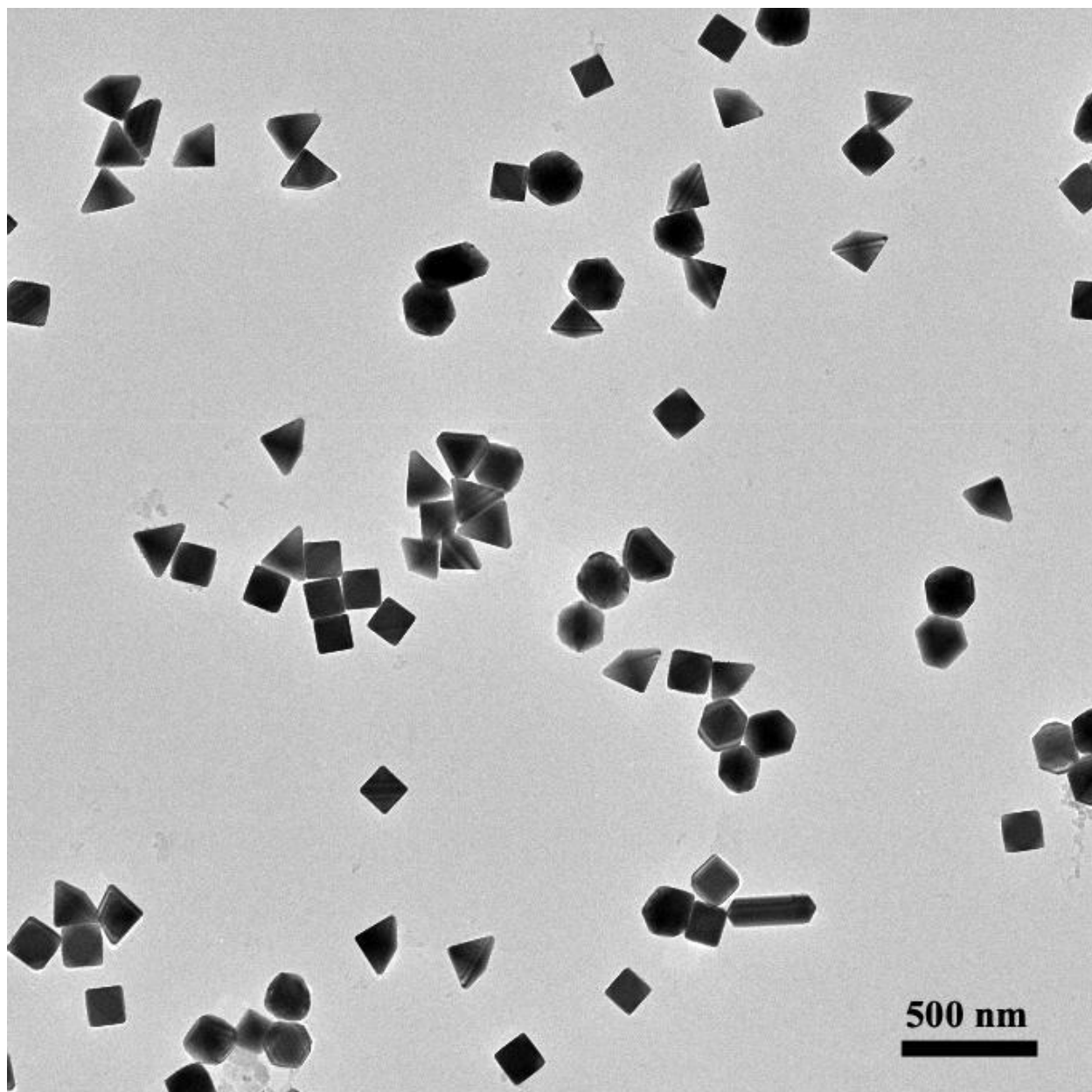


Figure S23. TEM image of Ag nanoparticle after full vertical growth of nanoplates with 6mL  $\text{AgNO}_3$  by using triangular silver nanoplate (78nm in length) as seeds. The ratio of the number of bipyramid to cube is near 1:1 (34:31).

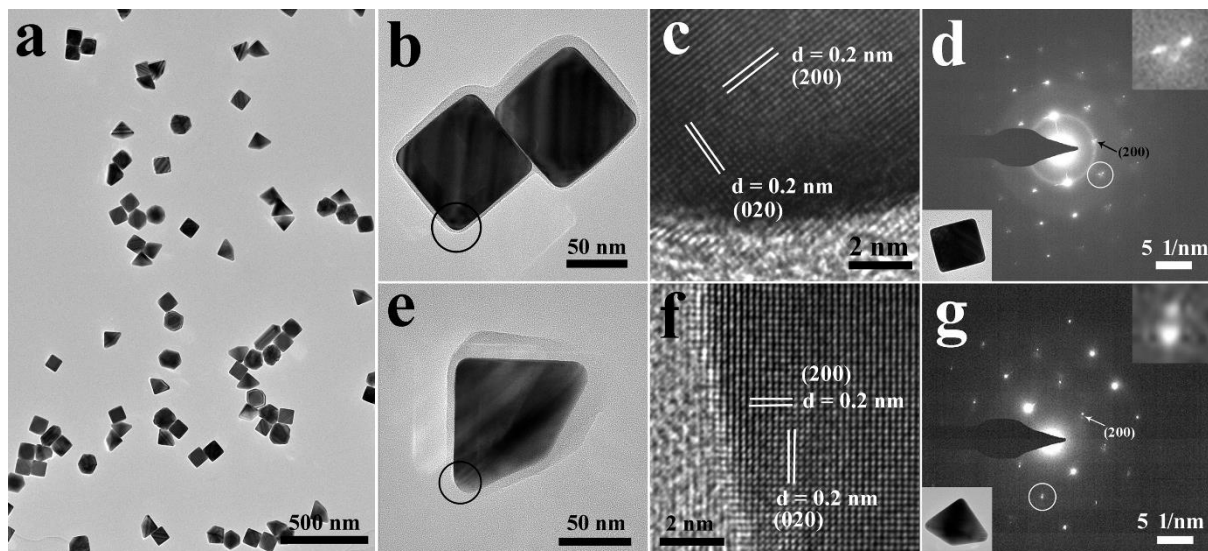


Figure S24. TEM analysis of silver nanoparticles after growth of triangular nanoplates with 6mL  $\text{AgNO}_3$ . (a) TEM image of Ag nanocubes and nanobipyramids. (b, c) TEM images of nanocubes and high-resolution (HR) TEM image at the corner signed by circle; (d) electron diffraction of a single cube (top inset is the enlarged diffraction spot marked by circle; bottom inset is corresponding cube). (e, f) TEM image of a nanobipyramid and HR-TEM image at the corner; (g) electron diffraction of a single nanobipyramid (top inset is the enlarged diffraction spot marked by circle; bottom inset is corresponding nanobipyramid). Multiple sets of spots in a single diffraction spot indicated presence of twined structure.

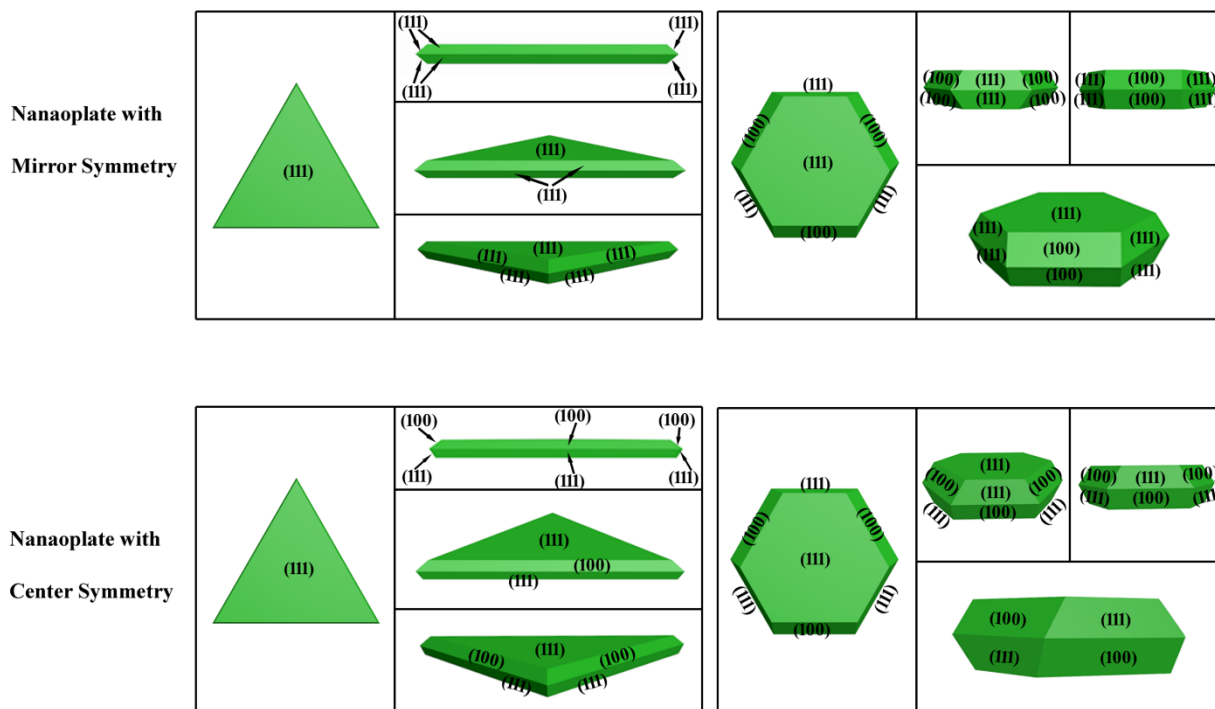


Figure S25. Geometric simulations of triangular and hexagonal nanoplates with different symmetry and corresponding faces arrangements. Nanoplates with mirror symmetry would have the same side facet (100) faces or (111) faces at the lateral directions. Nanoplates with center symmetry would have a pair of (100) face and (111) face at the lateral directions, with one below and one above the middle stacking faults.